Bifurcation theory of a 1-dimensional transport model for the L-H transition

W Weymiens,[1, a)] H J de Blank,[1] and G M D Hogeweij[1]
FOM Institute DIFFER – Dutch Institute for Fundamental Energy Research, Association EURATOM-FOM, Trilateral Euregio Cluster, PO Box 1207, Nieuwegein, The Netherlands

(Dated: 18 February 2014)

Transitions between low and high-confinement (L-H transitions) in magnetically confined plasmas can appear as three qualitatively different types: sharp, smooth, and oscillatory. Bifurcation analysis unravels these possible transition types and how they are situated in parameter space. In this paper the bifurcation analysis is applied to a 1-dimensional model for the radial transport of energy and density near the edge of magnetically confined plasmas. This phenomenological L-H transition model describes the reduction of the turbulent transport by $\mathbf{E} \times \mathbf{B}$-flow shear self-consistently with the evolution of the radial electric field. Therewith, the exact parameter space, including the threshold values of the control parameters, of the possible L-H transitions in the model is determined. Furthermore, a generalised equal area rule is derived to describe the evolution of the transport barrier in space and time self-consistently. Applying this newly developed rule to the model analysed in this paper reveals a naturally occurring transition to an extra wide transport barrier that may correspond to the improved confinement known as the very-high-confinement mode.

PACS numbers: 52.25 Fi, 52.25 Xz, 52.55 Dy, 52.55 Fa

I. INTRODUCTION

In 1982 the ASDEX team discovered the so called "High confinement mode" or "H-mode"[1], in which the energy confinement of a magnetically confined fusion plasma becomes, typically, twice as good (compared to the standard "Low confinement mode" or "L-mode"). Although this very beneficial, L- to H-mode transition has been seen in most present day tokamaks, all physical mechanisms which are relevant to these transitions are still not fully identified[2].

Many different models have been introduced[3,4] to explain the reduction of transport due to the L-H transition. Some models, based on sets of 0-dimensional dynamical equations, are well capable of qualitatively describing global temporal evolution behaviour around L-H transitions. However, they lack a description of the radial structure of the transport barrier. Since the improvements of diagnostic capabilities to observe highly spatially[2] and temporally[5,6] resolved edge profiles, there is a growing need for L-H transition models capable of predicting such spatial and temporal observations together with their threshold parameters. These 1-dimensionally extended models exist (e.g., Refs.[7–9]). However, their analysis was restricted to simulations of different dynamical behaviors without the determination of their full parameter space and their corresponding threshold boundaries. Bifurcation analysis, however, will give the exact boundaries in parameter space between different states and the different types of transitions between them, and is therefore very useful in analysing L-H transition models.

The nonlinear dynamics observed during L-H transitions can be identified as certain fundamental bifurcations. These bifurcations nicely organise the parameter space in different regimes for the different types of transitions, such as the sharp L-H and H-L transitions exhibiting hysteresis, the smooth transitions, and the oscillating transitions (called dithering or I-phase). Reference[10] gives the bifurcation theory for 1-dimensionally extended models that allow the characterisation of these typical bifurcations in a basic model for the L-H transition based on partial differential equations (PDEs). In this paper an advanced phenomenological 1-dimensional transport model for the L-H transition is analysed on the basis of this extended bifurcation theory. The bifurcations of the steady state profiles are characterised together with their corresponding control parameters and threshold values, which illustrates the robustness of the bifurcation structure of these kinds of models under substantial modifications.

The considered model is based on the transport of particles and heat along the minor radius of a magnetically confined fusion plasma. The L-mode radial transport is assumed to be dominated by turbulence. The influence of flows on turbulence is widely viewed as a mechanism able to reduce radial transport. More specifically, it is expected that the $\mathbf{E} \times \mathbf{B}$-flow, especially a shear in the $\mathbf{E} \times \mathbf{B}$-flow[11,18], is capable of tearing apart turbulent eddies. So, to model this effect properly it is necessary to include the evolution of the radial electric field and the corresponding flow profile. The small scale behaviour of the tearing of turbulence, and the possible back reaction of turbulence generating zonal flows is not contained in this model. The effect of the large scale radial electric field gradient (mean flow shear) on the turbulence, is modeled by effective transport coefficients that directly depend on the radial electric field shear. This phenomenological description of transport reduction is

[a)] w.weymiens@differ.nl

used often in literature[16?] , and has proven to be a useful simplification for H-mode modeling.

In general, nonlinear reaction diffusion systems can exhibit transition behavior. The spatial and temporal propagation of such transitions are analysed self-consistently, which leads to a generalised equal area rule. This newly developed rule could apply to all sorts of transition phenomena, such as flame front propagation or the propagation of signals in neurons. In this paper the generalised equal area rule is applied to the spatial and temporal evolution of the transport barrier[12,13] as is described by the considered model. This analysis leads to the natural arising of two different types of barrier width scalings. Right after the L-H transition the barrier width is set by the viscosity of the plasma, corresponding to a width in the order of a few gyro-radii. If the heating power is raised sufficiently, the barrier can grow inward, the growing width being determined by the generalised equal area rule. This growth of a larger transport barrier may be a natural description of the occurrence of a very-high-confinement mode (VH-mode) as observed in DIII-D[14] and JET[15], and it could occur naturally in some reaction diffusion systems with a certain general structure, the so-called S-curve models[7,16,17].

This paper is organised as follows. First of all, the 1-dimensional L-H transition model is described in Sec. II. In Sec. III, the relevant bifurcations for the L-H transition are identified and compared to the original model introduced by Zohm[8]. In Sec. 5, a generalised equal area rule is introduced to describe the growth of the pedestal. In Sec. V, this rule is applied to the considered model, and linked to the observation of VH-mode like states.

II. TRANSPORT MODEL FOR THE L-H TRANSITION

The degree of confinement is determined by the 1-dimensional transport in a tokamak along the minor radius of the torus, i.e., from the hot core of the toroidal plasma towards the colder edge. The radial transport of particles and heat is determined by the particle- and heat- fluxes, respectively, in the form of a continuity equation. We consider a layer near the edge of the plasma that is relatively thin compared to the plasma minor radius. We approximate this layer, just for conciseness, with a slab geometry, such that these equations become

$$\frac{\partial n}{\partial t} = -\frac{\partial \Gamma}{\partial r} \tag{1a}$$

$$\frac{\partial}{\partial t}\left(\frac{nT}{\gamma - 1}\right) = -\frac{\partial q}{\partial r} \tag{1b}$$

where we assume equal temperatures of the ions and electrons, and the absence of particle and heat sources inside the layer. The particle and heat fluxes are given by

$$\Gamma = -D\frac{\partial n}{\partial r} \tag{2a}$$

$$q = -\chi n\frac{\partial T}{\partial r} + \frac{\Gamma T}{\gamma - 1} \tag{2b}$$

The particle flux, Γ, is governed by some effective particle diffusion due to the anomalous transport of electrons and ions. The heat flux, q, is a combination of some effective radial thermal conduction and heat advection due to the net mass-flow described by the particle flux, with γ the adiabatic index. A change from low confinement to high confinement can therefore be described by a change in the transport coefficients; particle diffusivity, D, and heat conductivity χ. In L-mode the transport is dominated by turbulence. A well known effect in turbulent fluid dynamics is the reduction of turbulence by the generation of sheared flows[2], these flows can be externally driven or generated from the turbulence itself via, e.g., Reynolds stress leading to zonal flows[19]. An analogous self organisation mechanism could be responsible for the formation of the self-sustained transport barrier in fusion plasmas[20]. The turbulence quenching sheared flows in a plasma are identified as the $\mathbf{E}\times\mathbf{B}$-flows[22?,23]. These flow shears are indeed observed as driven by Reynolds stress in the form of zonal flows[3,24], and externally driven by probes generating a radial electric field[25], and by various other mechanisms. This quenching mechanism is frequently modelled[16?] as an effective diffusivity depending on the $\mathbf{E}\times\mathbf{B}$-flow shear,

$$D = D_{min} + \frac{D_{max} - D_{min}}{1 + \tilde{\alpha}(V'_{\mathbf{E}\times\mathbf{B}})^2}, \tag{3}$$

where the prime denotes the radial derivative, and the square of the flow shear expresses the fact that both signs of the flow shear can suppress turbu-lence[26]. A similar expression is used for the thermal conductivity only with constants; χ_{min} and χ_{max}. Since the $\mathbf{E}\times\mathbf{B}$-flow driven by a radial electric field can be approximated by, $V_{\mathbf{E}\times\mathbf{B}} \approx E_r/B$, the transport coefficients take the form of

$$D = D_{min} + \frac{D_{max} - D_{min}}{1 + \alpha Z'^2}, \tag{4}$$

where Z is the normalised radial electric field,

$$Z = \frac{\rho_p e E_r}{T_i}, \qquad \text{and} \qquad \rho_p = \frac{m v_{th}}{q B_p}. \tag{5}$$

Furthermore, we do not expect the L-H transition to be initiated by some specific difference between the two transport coefficients. Such that we can make the following simplification: $\chi = D/\zeta(\gamma - 1)$, with ζ a proportionality factor, leading to the following transport equations:

$$\frac{\partial n}{\partial t} = \frac{\partial}{\partial r}\left(D\frac{\partial n}{\partial r}\right) \tag{6a}$$

$$\frac{\partial}{\partial t}(nT) = \frac{\partial}{\partial r}\left[D\left(\frac{n}{\zeta}\frac{\partial T}{\partial r} + T\frac{\partial n}{\partial r}\right)\right] \tag{6b}$$

To model the evolution of the transport self-consistently it is necessary to include the evolution of the radial electric field explicitly[7,8,27]

$$\varepsilon\frac{\partial Z}{\partial t} = \mu\frac{\partial^2 Z}{\partial r^2} + c_n\frac{T}{n^2}\frac{\partial n}{\partial r} + \frac{c_T}{n}\frac{\partial T}{\partial r} - G(Z) \tag{6c}$$

where $\varepsilon = B_p^2/(B^2\nu_i)$ is the dielectric constant of the polarised plasma. The radial currents are caused by the anomalous shear viscosity of the $\mathbf{E}\times\mathbf{B}$-drift[28] (first term on the right-hand side (RHS) where $\mu \sim \rho_p^2$ is the ratio of viscosity to collision frequency). The second and third terms are due to the bipolar part of the anomalous cross field flux, i.e., the excess flux of electrons relative to that of ions[28]. Furthermore, additional radial current contributions may be generated due to a variety of mechanisms[16,29] that depend on the radial electric field itself, e.g., ion orbit losses[30,31], bulk viscosity[31,32] (due to the inhomogeneity of the magnetic field), the anomalous cross field flux[27,32], Reynolds stress, collisional processes (e.g., ripple diffusion, gyro viscosity), charge exchange[33,34], external current drive, etc., resulting in a function of the radial electric field with many terms, $G(Z)$. However, general bifurcation theory implies that the dynamics corresponding to the L-H transition occurs in the neighborhood of the cusp bifurcation[10]. This cusp-bifurcation transition behaviour can only occur around an inflection point of this nonlinear function of the radial electric field. Therefore, to describe the transition behaviour it is sufficient to Taylor expand this function of many terms around its inflection point to be able to describe its L-H transition behavior. The Taylor expansion around an inflection point at $Z = Z_s$ is

$$G(Z) \approx a + b(Z - Z_s) + (Z - Z_s)^3. \tag{7}$$

This closed set of coupled PDEs (Eqs. (6a, b, c)) is evaluated on a spatial domain that must be considerably larger than the size of the transport barrier to exclude boundary effects, but small enough that the core boundary stays away from the particle and heat sources in the core of the plasma. The outer edge of the plasma at the scrape-off layer (SOL) side is fixed at $r = 0$. The inner boundary of the considered spatial domain is located at $r = -\infty$, this is allowed because compared to the size of the transport barrier the inner boundary is far enough away. At this inner boundary all the particles and heat enters the system (there are no additional sources within the domain). These influxes can be used as control parameters of the system

$$\begin{aligned} \Gamma(r=-\infty) &= \text{constant} = \Gamma_{-\infty} \\ q(r=-\infty) &= \text{constant} = q_{-\infty} \\ Z'(r=-\infty) &= 0 \end{aligned} \tag{8}$$

At the other boundary of the system, i.e., the outer edge of the plasma, the temperature, density, and radial electric field are forced to drop toward zero with a certain e-folding length into the scrape-off layer,

$$\frac{T_e'}{T_e} = \frac{-1}{\lambda_T}, \qquad \frac{n_e'}{n_e} = \frac{-1}{\lambda_n}, \qquad \frac{Z_e'}{Z_e} = \frac{-1}{\lambda_Z}, \tag{9}$$

with constant gradient lengths λ_T, λ_n, and λ_Z of the same order of magnitude, and where from now on the subscript "e" is used for SOL edge values.

III. BIFURCATION ANALYSIS

The closed set of three PDEs (Eqs. (6a)-(6c)) with the six boundary conditions (Eqs. (8) and (9)) is the complete L-H transition model considered in this paper. This model greatly resembles the model introduced by Zohm[8] to explain the dithering behaviour during L-H transitions, now often called the I-phase. The only difference between both models is the description of the effective diffusivity. In this paper the transport is reduced due to a shear in the $\mathbf{E}\times\mathbf{B}$-flow (see Eq. (4)), in Zohm's model only the value of the radial electric field was taken into account (not its shear) in the following way:

$$D(Z) = \frac{D_{max} + D_{min}}{2} + \frac{D_{max} - D_{min}}{2}\tanh(Z) \tag{10}$$

The bifurcation analysis of Zohm's model was done in Ref.[10] and led to the following equation relating the steady state radial electric field profile to the steady state density profile:

$$-G(Z)D(Z) = \frac{T_{-\infty}D(Z_e)^2}{\Gamma_{-\infty}\lambda_n^2}(c_n\hat{n}^{-2} + c_g\hat{n}^{-\zeta-2}), \tag{11}$$

where $\hat{n} = n_0/n_{0e}$, is the steady state density normalised to its edge value, $n_{0e} = \Gamma_{-\infty}\lambda_n/D(Z_e)$. $T_{-\infty} = (\gamma - 1)q_{-\infty}/\Gamma_{-\infty}$ is the core boundary value of the steady state temperature, and $c_g = (\zeta c_T - c_n)/(1 + \zeta\lambda_T/\lambda_n)$. The derivation of Eq. (11) did not rely on the fact the diffusivity explicitly depended on the value of the radial electric field and not its shear, therefore it is still valid when we plug in the diffusivity depending on the shear of the radial electric field. Nevertheless, the RHS of Eq. (11) only depends on the radius via the density profile, that is a monotonic increasing function of the radius (starting from n_{0e} at $r = 0$ and increasing to infinity at $r = -\infty$). Therefore, the profile of the product $-G(Z)D(Z')$ will be a smooth monotonic function of the radius too, growing from zero at the core boundary to a constant value at the edge given by

$$-G(Z_e)D(Z_e') = (c_n + c_g)\frac{(\gamma-1)q_{-\infty}}{\Gamma_{-\infty}^2\lambda_n^2}D(Z_e')^2. \tag{12}$$

Making use of the Robin boundary condition for the radial electric field, $Z_e' = -Z_e/\lambda_Z$, allows both sides of Eq. (12) to be parameterised by Z_e, as is shown in Fig. 1(a). The slope, θ, of the tilted dashed line is determined by a specific combination of the constant parameters of the system

$$\theta = \frac{\Gamma_{-\infty}^2\lambda_n^2}{q_{-\infty}(\gamma-1)}\frac{1}{c_n + c_g}. \tag{13}$$

This specific value will then determine at which point both sides of Eq. (12) are equal, i.e., both lines intersect, and therewith the value of the transport coefficients at the edge of the plasma. Obviously, high values of θ will correspond to L-mode transport and lower values of θ will

correspond to H-mode transport. The L-H transition can thus be obtained by increasing, e.g., the heat flux coming from the core, $q_{-\infty}$, which is consistent with experiments. Additionally, other parameters can be used in this model to generate L-H transitions.

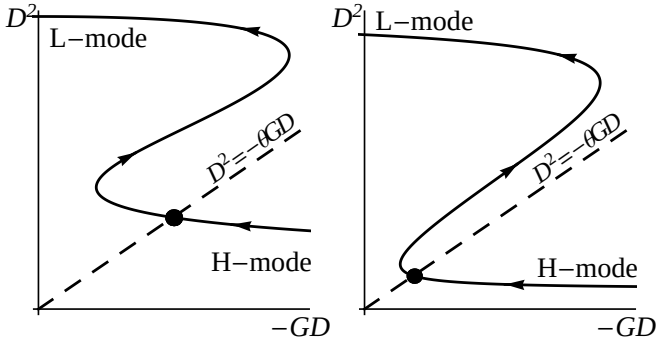

FIG. 1: The steady state solution at the edge of the plasma, Z_e, is determined by the intersection of the solid curve (parameterised by increasing Z_e along the arrows) with the tilted dashed line, as is dictated by Eq. (12). (a) $\mathbf{E}\times\mathbf{B}$-flow shear model of this paper, (b) Zohm's model for comparison[10].

In Fig. 1(b) the possible edge states of the radial electric field for Zohm's model are reproduced from Ref.[10]. The structure of the solutions of both models is qualitatively the same, and therefore the same arguments can be applied to find the bifurcations of this new model. A set of two fold bifurcations are recognised at the values of θ bounding the region with three intersections (i.e., coexistence of L-mode and H-mode solutions). These two different fold bifurcations make sure there is hysteresis between the L-H transition and the H-L transition. The Hopf bifurcations change the stability of these stationary solutions. Right before the L-mode or H-mode solution disappears (at the fold bifurcation), it already becomes unstable (at the Hopf bifurcation, where the slope of the curved solid line is vertical). Thus, eventually the L-H transition will occur at the Hopf-bifurcation threshold for θ. However, if the H-mode is not yet stable (i.e., it did not have its Hopf-bifurcation yet) the system will not have a stable steady state solution and will start to oscillate.
This stable limit cycle, shown in Fig. 2, consists of a fast transition where the radial electric field changes on a timescale of $\mathcal{O}(\varepsilon)$. The system then tries to relax towards an H-mode profile on a diffusive timescale. However, it thus reaches the other Hopf bifurcation, where the radial electric field suddenly jumps back towards L-mode values, and subsequently the profiles adapt to these values on a diffusive timescale. Thus the whole period of the limit cycle consists of two diffusive parts and two fast jumps. The bifurcation boundaries in parameter space determine the exact thresholds between the different types of dynamics. In Fig. 3, the parameter space of both the $\mathbf{E}\times\mathbf{B}$-flow shear model and Zohm's model is

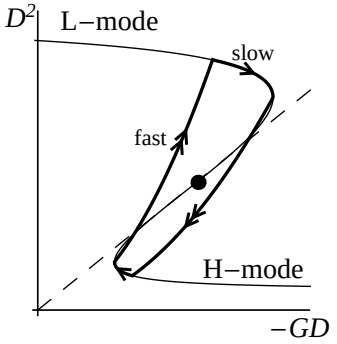

FIG. 2: For this value of θ the intersection occurs in the regime without stable stationary states at the edge of the plasma. Without those the system will oscillate according to a stable limit cycle, as is created by the Hopf bifurcation.

plotted, with the same values of the parameters. By comparing both parameter spaces of Fig. 3, one can immediately notice the different sizes of the limit cycle regions. So, in Zohm's model that describes only a flow (not the

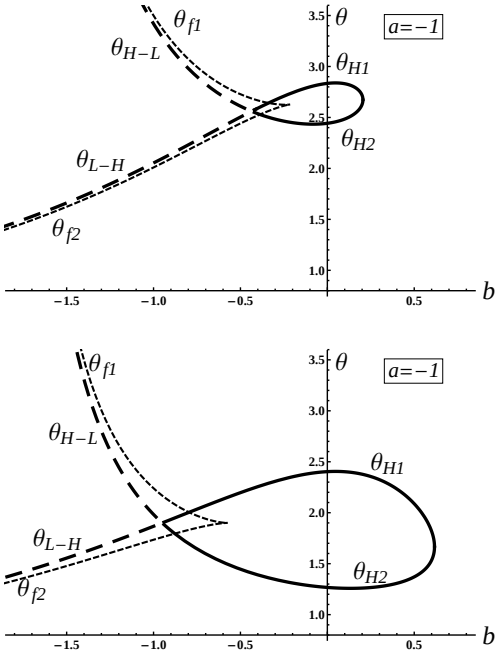

FIG. 3: The (b,θ)-parameter space for fixed $a<0$ of (a) $\mathbf{E}\times\mathbf{B}$-flow shear model of this paper, and (b) Zohm's model[10]. The cusp-shaped short-dashed lines indicate the fold bifurcations (θ_{f1} and θ_{f2}). The Hopf bifurcations consist of two parts, the dashed lines (θ_{L-H} and θ_{H-L}) lead to the sharp L-H and H-L transitions. At θ_{H1} and θ_{H2} the Hopf bifurcations are in reversed order, such that in the region surrounded by the solid curve only limit cycle solutions are possible.

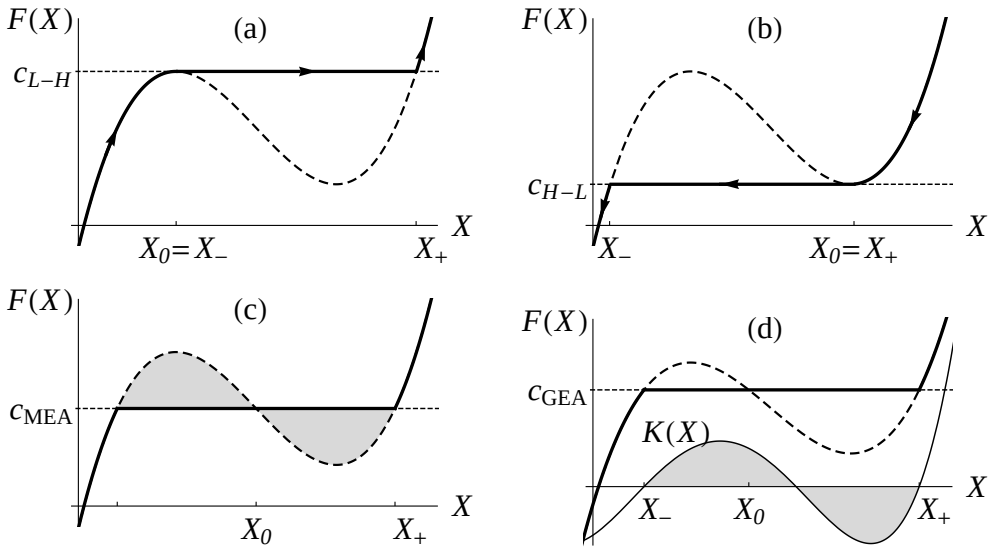

FIG. 4: (a) Maximal Hysteresis ($\mu \to 0$): L-H transition. (b) Maximal hysteresis ($\mu \to 0$): H-L transition. (c) Maxwell's equal area rule ($\varepsilon \to 0$). (d) Generalised equal area rule ($\mu \ll 1$, $\varepsilon \ll 1$), where the relation between $K(X)$ and $F(X)$ is given in Eq. (18).

shear) the oscillations during an oscillatory L-H transition will last a lot longer than in the flow-shear model, when the heating power is ramped-up at the same rate. Beside this, the onset of the oscillatory behaviour in Fig. 3(b) is at values of the heating power at which the flow shear model would have past the oscillatory behaviour and went into H-mode already. Additionally, one can see that the values for θ_{L-H} are generally higher (i.e., lower heating power threshold) for the flow-shear model, consistent with the believe that sheared flow is more efficient in reducing turbulence than a flow without shear.

IV. THE TRANSPORT BARRIER: SPACE AND TIME CONSISTENTLY

In this model the radial electric field is the main bifurcating variable of the model, that is similar to a three-component reaction diffusion system of the FitzHugh-Nagumo type. In general, these reaction diffusion systems have multiple stationary states and sharp transitions between them. These transitions can occur in time and space. The temporal transitions are regulated by a first order derivative, and the spatial transitions are regulated by a second order derivative,

$$-\varepsilon\frac{\partial X}{\partial t} + \mu\frac{\partial^2 X}{\partial r^2} = F(X) - c(r,t), \qquad (14)$$

where $F(X)$ is a nonlinear function, such that the RHS can have up to three roots (X_-, X_0, and X_+) depending on the value of the control parameter $c(r,t)$ that can be any continuous function of space and time. This form is generally valid for reaction diffusion systems of the FitzHugh-Nagumo type, however, in the following derivation the transitions between the roots are discussed in terms of the L-H transition to make the understanding of the applicability easier. Temporal transitions between the roots correspond to the sudden jumps from L-mode to H-mode and back, and the spatial transition occur when the core of the plasma exhibits L-mode like transport and the edge region exhibits H-mode like transport.

The limit of purely temporal transitions, and the limit of purely spatial transitions are well-known. In the limit of $\mu \to 0$ there is only a first order derivative of time, leading to a maximal hysteresis rule[13] for the temporal transition at threshold values of the control parameter c, at c_{L-H} and c_{H-L}, see Figs. 4(a) and 4(b). The other well known limit is $\varepsilon \to 0$, this limit describes with a second derivative in space how a high transport core can be connected to a low transport edge solution. In this time independent case the equation can be integrated over space once to give

$$\frac{dX}{dr} = \sqrt{\frac{2}{\mu}\int_{X_-}^{X}\Big(F(X) - c\Big)dX} \qquad (15)$$

which must vanish at X_+, leading to the Maxwell's equal area (MEA) rule[13,16],

$$\int_{X_-}^{X_+}\Big(F(X) - c_{MEA}\Big)dX = 0, \qquad (16)$$

where c_{MEA} is defined to be that value such that the integral vanishes, as is shown in Fig. 4(c), note that X_- and X_+ depend on the value of the control parameter too. For the consideration of the entire system consistently we assumed that the jumps in time and in space are rapid

(ε and μ are small), such that the transitions happen in an almost 1-dimensional zone in (r,t)-space, where the tangent to the zone is given by $dr/dt = -v$. This helps to treat both derivatives on the same footing: $d/dt \to v\ d/dr$, leading to the solution

$$\frac{dX}{dr} = \sqrt{\frac{2}{\mu}\int_{X_-}^{X} K(X)\ dX}, \tag{17}$$

where the new function $K(X)$ must satisfy:

$$K(X) - \varepsilon v\sqrt{\frac{2}{\mu}\int_{X_-}^{X} K(X)\ dX} = F(X) - c_{GEA}, \tag{18}$$

where c_{GEA} is defined such that the following integral vanishes,

$$\int_{X_-}^{X_+} K(X)dX = 0 \tag{19}$$

This is the generalised equal area (GEA) rule for the combined spatiotemporal transition from X_- to X_+, that is visualised in Fig. 4(d). Note that $K(X_-) = K(X_+) = 0$ but $K(X_0) \neq 0$ differs from $F(X_0) = c_{GEA}$ by the square root of its integral. The GEA rule determines the position in space and time of the transition between L-mode transport and H-mode transport corresponding to the temporal growth of the barrier region. In Fig. 5 the area in space and time which will exhibit H-mode behaviour, i.e., the edge transport barrier, is given as function of the control parameter $c(r,t)$. The black line surrounding the H-mode region is given by $c = c_{GEA}$ which depends on the local slope v. This nondecreasing function, $c_{GEA}(v)$, has special values $c_{GEA}(-\infty) = c_{H-L}$, $c_{GEA}(0) = c_{MEA}$, and $c_{GEA}(\infty) = c_{L-H}$.

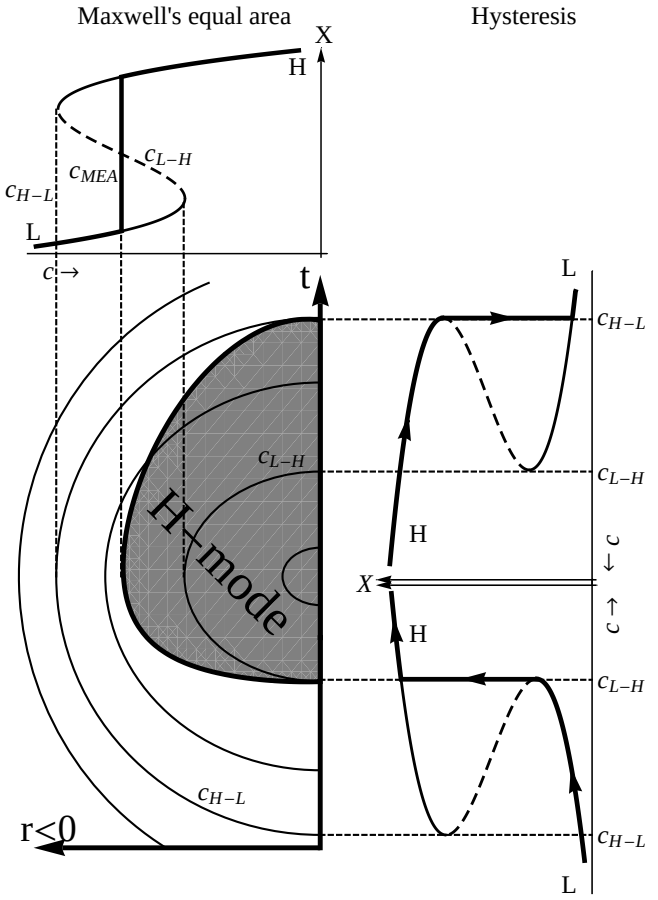

FIG. 5: A contour plot of the control parameter $c(r,t)$ in space and time, in which the special contours $c = c_{L-H}$ and $c = c_{H-L}$ are indicated. The asymmetric thick contour corresponds to the generalised equal area rule, $c = c_{GEA}$ (Eq. (18)), bounding the region in (r,t) that exhibits H-mode transport. c_{GEA} depends on the local slope $v = -dr/dt$ and has special values: $c_{GEA}(v = \infty) = c_{L-H}$, $c_{GEA}(v = 0) = c_{MEA}$, and $c_{GEA}(v = -\infty) = c_{H-L}$.

V. TWO DIFFERENT REGIMES IN TRANSPORT BARRIER SIZES

In this section we apply the GEA rule to Zohm's model, because it is possible analytically, and it leads to specific diffusivity profiles as plotted in Figs. 6(b)-6(f), which may help the understanding. With the use of Eq. (11), we can rewrite the evolution equation of the radial electric field, eq. (6c), in almost the same form as Eq. (14)

$$-\varepsilon\frac{\partial Z}{\partial t} + \mu\frac{\partial^2 Z}{\partial r^2} = G(Z) + \frac{f(\hat{n})}{D(Z)} \tag{20}$$

where $f(\hat{n})$ is a pure function of the normalised steady state density, but more importantly is always independent of Z. The RHS of this equation is just slightly different than the RHS of Eq. (14), which makes it possible that this system can have two different regimes of

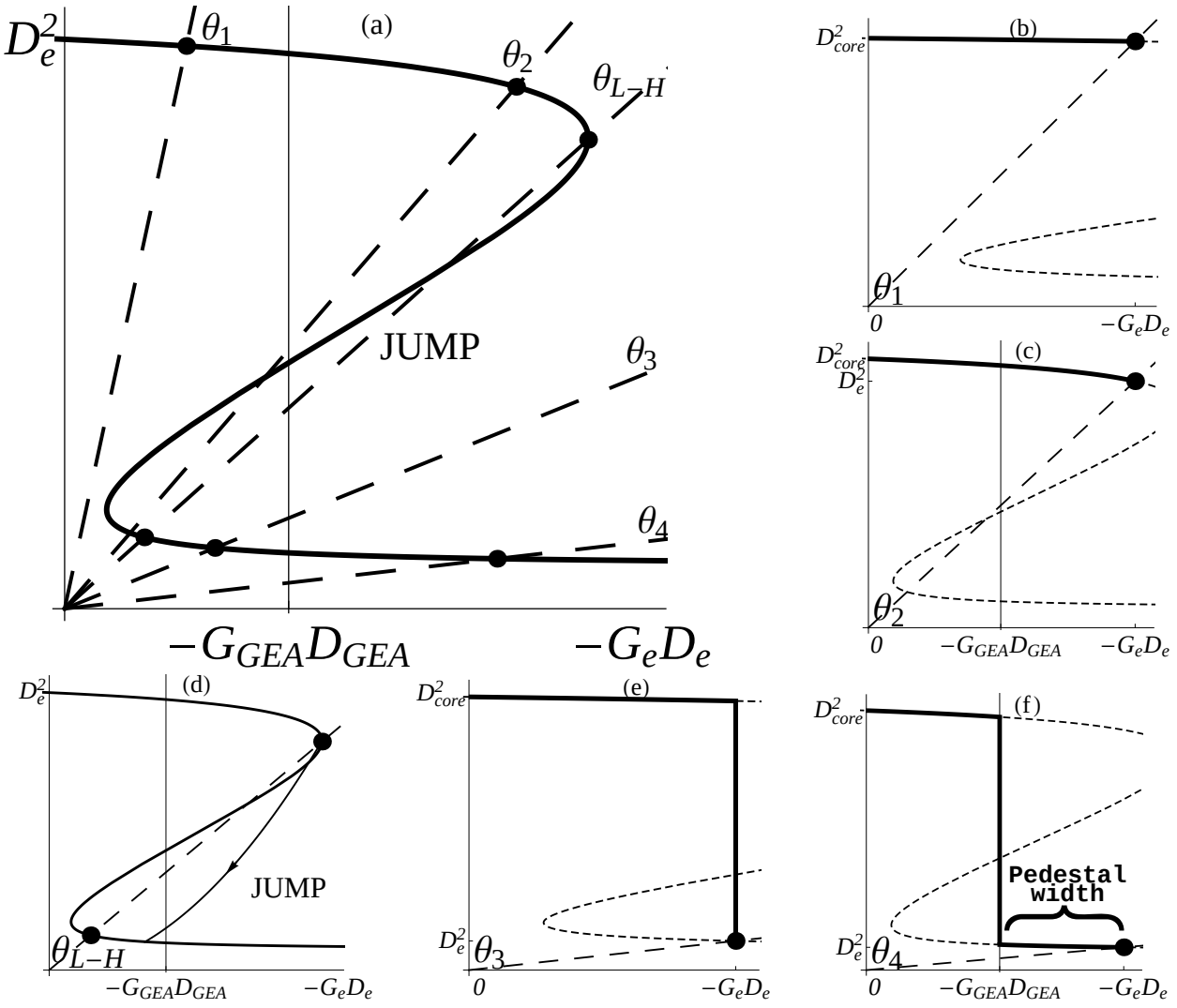

FIG. 6: (a) The edge steady state solutions of Zohm's model for different values of the control parameter, θ. The profiles corresponding to these edge solutions are indicated in the surrounding graphs together with the jump trajectory during the L-H transition. The profiles are drawn from $r = -\infty$ (i.e., $-GD = 0$) with diffusivity D_{core} to the edge at $r = 0$ (i.e., $-GD = -G_eD_e$) with diffusivity D_e. (b) $\theta = \theta_1$, L-mode: The profile of the diffusivity squared which is almost constant over the entire spatial region. (c) $\theta = \theta_2$, L-mode: Approaching the L-H transition D_e will slightly drop. (d) $\theta = \theta_{L-H}$, The L-H transition: At the threshold value the Hopf bifurcation makes the L-mode unstable and the system jumps to the stable H-mode branch following the indicated trajectory; $G = constant$. (e) $\theta = \theta_3$, *"thin-barrier H-mode:"* The edge state did not yet exceed the GEA-threshold, Eq. (25). The barrier width is set by the viscosity, i.e., of the order of an ion gyro-radius. (f) $\theta = \theta_4$, *"thick-barrier H-mode:"* profile with an enlarged pedestal, whose width is set by the GEA rule.

transport barrier sizes as will become clear in this section. The MEA rule would dictate a transition from Z_- to Z_+ for such a value of $f(\hat{n})$ that the following integral vanishes:

$$\int_{Z_-}^{Z_+} G(Z) + \frac{f_{MEA}}{D(Z)} dZ = 0 \qquad (21)$$

where Z_- and Z_+ are roots of the RHS of Eq. (20) with $f(\hat{n}) = f_{MEA}$ such that

$$-G(Z_-)D(Z_-) = -G(Z_+)D(Z_+) = f_{MEA} \qquad (22)$$

However, the GEA rule dictates a slightly different value of $f(\hat{n})$, namely, such a value that the solution of

$$K(Z) - \varepsilon v \sqrt{\frac{2}{\mu} \int_{Z_-}^{Z} K(Z) dZ} = G(Z) + \frac{f_{GEA}}{D(Z)}, \qquad (23)$$

for $K(Z)$, has a vanishing integral

$$\int_{Z_-}^{Z_+} K(Z) dZ = 0, \qquad (24)$$

where Z_- and Z_+ are roots of the RHS of Eq. (20) with $f(\hat{n}) = f_{GEA}$. This leads to a slightly different transition criterium,

$$-G(Z_-)D(Z_-) = -G(Z_+)D(Z_+) = f_{GEA}. \qquad (25)$$

Thus, if Z_e passes a certain threshold value the GEA rule predicts that the transition moves inwards into the plasma starting out from the edge. It may occur that when this requirement is not yet fulfilled the intersection in Fig. 1 is already on the low diffusivity side, indicating that the edge state of the plasma has H-mode transport. This would lead to a profile of the radial electric field having an L-mode value in the entire spatial domain all the way up to the edge, where it jumps to an H-mode value only at this edge boundary. However, for finite viscosity, $\mu \neq 0$, this region is not infinitely thin, but of the order of the viscosity. Only when θ is decreased even further until the edge value of the radial electric field is such that the GEA requirement is fulfilled, then the transition starts to move inward towards a much wider transport barrier, as is shown in Fig. 5. In Fig. 6, an example is shown of such a transition, where the system has to go through a regime of a thin transport barrier set by the viscosity before the transport barrier can grow inwards according to the GEA rule. In panel (a) the decrease of the control parameter simulating an L-H transition is indicated with the sequence $\theta_1 \rightarrow \theta_2 \rightarrow \theta_3 \rightarrow \theta_4$. The corresponding steady state profiles of the diffusivity squared are shown in the surrounding panels, where the intersections (indicated with the black dots) determine the value of $-GD$ at the edge. In panels b and c the system is still in L-mode. When the threshold $\theta = \theta_{L-H}$ is met the Hopf bifurcation will make the L-mode solution unstable and the system will jump towards the only stable stationary state that is left. This very fast transition (of the order of ε) occurs along the lines of constant $G(Z)$ as is indicated by the arrow in panel (d). This is because on this very fast timescales the edge temperature and density cannot adapt, such that $G(Z)$ is not allowed to change too. However, the end point of the jump does not necessarily coincide with the edge stationary state dictated by the slope θ. Therefore, the system will evolve on a transport timescale until the new stationary state is reached. This new stationary state has an H-mode value at the edge, although the GEA condition, Eq. (25), is not yet fulfilled. The corresponding profile in this *thin-barrier H-mode* regime is plotted in panel (e). Only when θ is decreased so far that the intersection has crossed the GEA condition, then the transition moves into the plasma to build a *thick-barrier H-mode* as is shown in panel (f). So there are two different regimes of barrier thickness, the thick barrier has a width increasing with the input power, while the thin barrier has a constant width as function of the heating power. In the limit of small μ, we can assume that Z increases linearly from Z_- towards Z_+, with $dZ/dr \propto (Z_+ - Z_-)/\sqrt{\mu}$. If we define the end of the barrier to be the point where the diffusivity is closer to L-mode values than to H-mode values ($Z = 0$ in the case of Zohm's model), than it leads to a barrier width proportional to $\sqrt{\mu}\frac{-Z_-}{(Z_+ - Z_-)}$.

VI. CONCLUSION AND DISCUSSION

Bifurcation analysis is a powerful tool to compare the qualitative transition behaviour of proposed L-H transition models. The model analysed in this paper is based on the reduction of transport due to $\mathbf{E} \times \mathbf{B}$-flow shear combined with the transport equations for heat and particles, and the evolution of the radial electric field. The bifurcations found in this system of PDEs showed the organisation in parameter space of the three types of L-H transitions that are observed in magnetically confined fusion plasmas. Mostly observed in experiments is the sharp transition exhibiting hysteresis between the forward L-H transition and the backward H-L transition. Furthermore, there is the smooth transition from L-mode to H-mode and back. Additionally, a region in parameter space is identified with oscillatory transitions, like the dithering or I-phase. Since the qualitative bifurcation structure is the same as the one of Zohm's original model[8], it illustrates that this bifurcation structure is robust under substantial modifications. It would be interesting to further investigate how the bifurcation structure will or will not change with additional physics. The evolution of the turbulence itself and its interaction with zonal flows, like the 0-D variant introduced in Ref.[35], would be a relevant extension. Recently, a paper was published[36] which proposes such a combination of the 1-D transport equations with the evolution of the turbulence and zonal flows, and is probably suitable for investigation with our bifurcation analysis.

Furthermore, the full analysis of the spatial and temporal evolution of the transport barrier self consistently revealed a natural description of another type of transition. After the L-H transition a *thin-barrier H-mode* is created having a width of the order of the viscosity (approximately several gyro-radii). Thereafter, if the heating power is increased further, another threshold may be met, namely, GEA condition, Eq. (25). This GEA rule than describes the growth of an extra wide pedestal, the *thick-barrier H-mode*. This enlarged pedestal regime might be the mechanism responsible for the VH-mode observed in DIII-D[14] and JET[15]. This mechanism described in this paper is quite generally valid for bifurcating transport models (related to so-called S-curve models); however, a tokamak plasma might already reach some other limits (e.g., density limit, edge localized modes (ELMs) and disruptions) before the required heating power is reached. Since these effects are not incorporated in this model, we do not claim to have found a direct way to reach a VH-mode state.

ACKNOWLEDGEMENTS

This work, supported by the European Communities under the contract of Association between EURATOM/FOM, was carried out within the framework of the European Fusion Programme with financial support from NWO. The views and opinions expressed herein do not necessarily reflect those of the European Commission. This work is supported by NWO-RFBR Centre-of-Excellence on Fusion Physics and Technology (Grant nr. 047.018.002)

REFERENCES

[1] Wagner F, Becker G, Behringer K, Campbell D, Eberhagen A, Engelhardt W, Fussmann G, Gehre O, Gernhardt J, v Gierke G, Haas G, Huang M, Karger F, Keilhacker M, Klüber O, Kornherr M, Lackner K, Lisitano G, Lister G G, Mayer H M, Meisel D, Müller E R, Murmann H, Niedermeyer H, Poschenrieder W, Rapp H, Röhr H, Schneider F, Siller G, Speth E, Stäbler A, Steuer K H, Venus G, Vollmer O and Yü Z 1982 *Phys. Rev. Lett.* **49**(19) 1408–1412

[2] Wagner F 2007 *Plasma Physics and Controlled Fusion* **49** B1

[3] Diamond P H, Hasegawa A and Mima K 2011 *Plasma Physics and Controlled Fusion* **53** 124001

[4] Terry P W 2000 *Rev. Mod. Phys.* **72**(1) 109–165

[5] Conway G D, Angioni C, Ryter F, Sauter P and Vicente J (ASDEX Upgrade Team) 2011 *Phys. Rev. Lett.* **106**(6) 065001

[6] Estrada T, Hidalgo C, Happel T and Diamond P H 2011 *Phys. Rev. Lett.* **107**(24) 245004 and references therein

[7] Itoh S I, Itoh K, Fukuyama A and Miura Y 1991 *Phys. Rev. Lett.* **67**(18) 2485–2488

[8] Zohm H 1994 *Phys. Rev. Lett.* **72**(2) 222–225

[9] del Castillo-Negrete D, Carreras B A and Lynch V E 2004 *Plasma Physics and Controlled Fusion* **46** A105

[10] Weymiens W, de Blank H J, Hogeweij G M D and de Valenca J C 2012 *Physics of Plasmas* **19** 072309 (pages 10)

[11] Schmitz L, Zeng L, Rhodes T L, Hillesheim J C, Doyle E J, Groebner R J, Peebles W A, Burrell K H and Wang G 2012 *Phys. Rev. Lett.* **108** 155002

[12] Diamond P H, Lebedev V B, Newman D E and Carreras B A 1995 *Physics of Plasmas* **2** 3685–3695

[13] Lebedev V B and Diamond P H 1997 *Physics of Plasmas* **4** 1087–1096

[14] Jackson G L, Winter J, Taylor T S, Burrell K H, DeBoo J C, Greenfield C M, Groebner R J, Hodapp T, Holtrop K, Lazarus E A, Lao L L, Lippmann S I, Osborne T H, Petrie T W, Phillips J, James R, Schissel D P, Strait E J, Turnbull A D, West W P and Team D D 1991 *Phys. Rev. Lett.* **67**(22) 3098–3101

[15] Greenfield C M, Balet B, Burrell K H, Chu M S, Cordey J G, DeBoo J C, Deliyanakis N, Doyle E J, Groebner R J, Jackson G L, Konoshima S, O'Brien D P, Porte L, Rettig C L, Osborne T H, John H S, Sips A C C, Staebler G M, Strait E J, Stubberfield P M, Taylor T S, Thompson S J, Thomsen K and Turnbull A D 1993 *Plasma Physics and Controlled Fusion* **35** B263

[16] Connor J W and Wilson H R 2000 *Plasma Physics and Controlled Fusion* **42** R1

[17] Malkov M A and Diamond P H 2008 *Physics of Plasmas* **15** 122301 (pages 16)

[18] Burrell K H 1997 *Physics of Plasmas* **4** 1499–1518

[19] Shukla P and Stenflo L 2003 *Physics Letters A* **307** 154 – 157 ISSN 0375-9601

[20] Marcus P S, Kundu T and Lee C 2000 *Physics of Plasmas* **7** 1630–1640

[21] Burrell K H, Doyle E J, Gohil P, Groebner R J, Kim J, Haye R J L, Lao L L, Moyer R A, Osborne T H, Peebles W A, Rettig C L, Rhodes T H and Thomas D M 1994 *Physics of Plasmas* **1** 1536–1544

[22] Burrell K H 1999 *Physics of Plasmas* **6** 4418–4435

[23] Punzmann H and Shats M G 2004 *Phys. Rev. Lett.* **93**(12) 125003

[24] Fujisawa A 2009 *Nuclear Fusion* **49** 013001

[25] Taylor R J, Brown M L, Fried B D, Grote H, Liberati J R, Morales G J, Pribyl P, Darrow D and Ono M 1989 *Phys. Rev. Lett.* **63**(21) 2365–2368

[26] Biglari H, Diamond P H and Terry P W 1990 *Physics of Fluids B: Plasma Physics* **2** 1–4

[27] Itoh S I and Itoh K 1988 *Phys. Rev. Lett.* **60**(22) 2276–2279

[28] Itoh K and Itoh S I 1996 *Plasma Physics and Controlled Fusion* **38** 1

[29] Itoh K 1994 *Plasma Physics and Controlled Fusion* **36** A307

[30] Hinton F L and Chu M S 1985 *Nuclear Fusion* **25**(3) 345

[31] Shaing K C and Crume E C Jr 1989 *Phys. Rev. Lett.* **63** 2369

[32] Hassam A B, Antonsen T M Jr, Drake J F and Liu C s 1991 *Phys. Rev. Lett.* **66** 309

[33] Itoh K and Itoh S-I 1995 *Plasma Physics and Controlled Fusion* **37** 491

[34] D'ippolito D A and Myra J R 2002 *Physics of PLasmas* **9** 853

[35] Kim E-j and Diamond P H 2003 *Phys. Rev. Lett.* **90**(18) 185006

[36] Miki K, Diamond P H, Gürcan Ö D, Tynan G R, Estrada T and Schmitz L 2012 *Physics of Plasmas* **19** 092306